Conditioned Pain Modulation affects the withdrawal reflex pattern to nociceptive stimulation in humans

Jure, Fabricio Ariel; Arguissain, Federico; Biurrun Manresa, José; Andersen, Ole Kæseler

Published in:
Neuroscience

DOI (link to publication from Publisher):
10.1016/j.neuroscience.2019.04.016

Publication date:
2019

Document Version
Accepted author manuscript, peer reviewed version

Conditioned Pain Modulation affects the withdrawal reflex pattern to nociceptive stimulation in humans

Fabricio Ariel Jure [a], Federico Gabriel Arguissain [a, b, c], José Alberto Biurrun Manresa [b, d], Ole Kæseler Andersen * [a, b]

[a] Integrative Neuroscience, SMI®, Dept. of Health Science and Technology, Fredrik Bajers Vej 7, Aalborg Ø (9220), Aalborg, Denmark

[b] Center for Neuroplasticity and Pain (CNAP), SMI®, Dept. of Health Science and Technology, Fredrik Bajers Vej 7, Aalborg Ø (9220), Aalborg, Denmark

[c] Hammel Neurorehabilitation and Research Centre, Aarhus University Hospital, Voldbyvej 15, Hammel (8450), Denmark

[d] Institute for Research and Development in Bioengineering and Bioinformatics (IBB), CONICET-UNER, Ruta 11 km. 10, Oro Verde (3100), Argentina

E-mails: faj@hst.aau.dk, fga@hst.aau.dk, jbiurrun@hst.aau.dk, oka@hst.aau.dk

*Corresponding author:

Professor Ole Kæseler Andersen, dr. scient., Ph.D.

Phone: +45 9940 8816

E-mail: oka@hst.aau.dk

Address: Aalborg University, Faculty of Medicine, Dep. of Health Science and Technology, Fredrik Bajers Vej 7, 9220 Aalborg Ø, Aalborg, Denmark

Abbreviations

BF: biceps femoris

CPM: conditioned pain modulation

CPT: cold-pressor test

CS: conditioning stimulus

EMG: electromyographic

NWR: nociceptive withdrawal reflex

RF: rectus femoris

RTh: reflex threshold

SOL: soleus

TA: tibialis anterior

ABSTRACT

Human studies have repeatedly shown that conditioning pain modulation (CPM) exerts an overall descending inhibitory effect over spinal nociceptive activity. Previous studies have reported a reduction of the nociceptive withdrawal reflex (NWR) under CPM. Still, how descending control influences the muscle activation patterns involved in this protective behavior remains unknown. This study aimed to characterize the effects of CPM on the withdrawal pattern assessed by a muscle synergy analysis of several muscles involved in the lower limb NWR. To trigger descending inhibition, CPM paradigm was applied using the cold-pressor test (CPT) as conditioning stimulus. Sixteen healthy volunteers participated. The NWR was evoked by electrical stimulation on the arch of the foot before, during and after the CPT. Electromyographic (EMG) activity of two proximal (rectus femoris and biceps femoris) and two distal (tibialis anterior and soleus) muscles were recorded. A muscle synergy analysis was performed on the decomposition of the EMG signals, based on a non-negative matrix factorization algorithm. Results showed that two synergies (Module I and II) were sufficient to describe the NWR pattern. Under CPM, Module I activation amplitude was significantly reduced in a narrow time-window interval (118-156ms) mainly affecting distal muscles, whereas Module II activation amplitude was significantly reduced in a wider time-window interval (150-250ms), predominantly affecting proximal muscles. These findings suggest that proximal muscles are largely under supraspinal control. The descending inhibitory drive exerted onto the spinal cord may adjust the withdrawal pattern by differential recruitment of the muscles involved in the protective behavior.

Keywords: nociceptive withdrawal reflex; electrical stimulation; cold-pressor test; withdrawal pattern; muscle synergy.

INTRODUCTION

Limb withdrawal is a vital protective behavior in response to potential tissue damage. This involuntary body reaction to noxious stimuli is carried out through spontaneous spinal reflexes, which allow a quick retraction of the affected area from actual or potential danger. This reflex, named nociceptive withdrawal reflex (NWR), is encoded in polysynaptic neuronal pathways at spinal level and it ends in the motor neurons of the muscles that produce the withdrawal pattern (Sandrini et al., 2005).

It is very well established that several intrinsic and extrinsic factors can modulate the overall NWR response. For example, changes of limb posture (Hagbarth and Finer, 1963), stimulation site (Andersen et al., 1999), gait phase (Spaich et al., 2006; Richard et al., 2015) and psychological states (Anon, n.d.; Bjerre et al., 2011; Bartolo et al., 2013) can alter dynamically the NWR. In particular, an important mechanism of spinal modulation is the conditioning pain modulation (CPM), a phenomenon in which the behavioral response to a painful stimulus is inhibited by another heterotopic painful stimulus (Kennedy et al., 2016) most likely via modulation of the descending drive onto spinal nociceptive pathways (Heinricher et al., 2009). This central mechanism inhibits noxious inputs to reduce the adverse effect of pain in potentially dangerous circumstances (Millan, 2002). Alterations of CPM have been associated with the development of chronic pain (Lewis et al., 2012).

Studies in humans have repeatedly shown that CPM exerts a descending inhibitory effect over the NWR activity (Willer et al., 1984, 1989; Le Bars et al., 1991; Terkelsen et al., 2001; Serrao et al., 2004; Biurrun Manresa et al., 2014). These previous reports have described the effect of CPM by characterizing the overall NWR response in terms of single muscle activity. Although this approach provides insights into the effect of CPM on the overall NWR, it gives little information on how descending modulatory pathways influence the muscle activation patterns involved in this protective behavior. This becomes relevant if the withdrawal reaction is considered as a net combination of several muscles acting across several joints. In fact, each muscle plays a different role in the overall withdrawal (Andersen et al., 2001). It is therefore plausible that the descending control exerts differential modulation that is dependent on the specific role of each muscle involved in the NWR (Kalliomäki et al., 1992).

In this regard, Sherrington (1910) was the first to describe this defensive reaction in animals as a stereotyped ‘flexion reflex’. Since then, studies in humans have demonstrated that the NWR

involves a combination of flexor and extensor muscles acting across several joints (Eklund et al. 1959; Hagbarth 1960; Kugelberg et al. 1960; Grimby 1963). Studies in animals (Schouenborg and Weng, 1994; Schouenborg, 2002) and later in humans (Andersen et al., 1999; Sonnenborg et al., 2001) have indicated that the NWR has a modular organization, where the optimal withdrawal movement away from the stimulus is the net result of the activation of independent reflex modules. Each individual reflex module consists of a specific cutaneous area called reflex receptive field (RRF) and a single muscle or a group of few synergistic muscles (Schouenborg, 2002).

Other reports in animals have provided evidence that the withdrawal response due to cutaneous stimulation of a particular site can be generated by a combination of specific muscle activation patterns, named muscle synergies (Tresch et al., 1999). These authors suggests that the central nervous system generates a repertoire of motor movements through a linear combination of different muscle synergies specified by networks in the spinal cord and/or brainstem (Bizzi et al., 2002, 2008), and the NWR pathways might thus make use of these spinal networks.

Hence, the aim of the study was to characterize the withdrawal pattern of the lower limb in humans during CPM. It is hypothesized that the different muscles involved in the NWR pattern are subjected to a differential descending modulatory control, reflecting the presence of withdrawal priorities across the joints of the lower limb. It would be then plausible to consider this defensive reaction as a complex hierarchized mechanism, possibly commanded by shared neural drives. Particularly, proximal and distal muscles might be differentially recruited due to the specific function of each muscle acting across joints. To this end, a muscle synergy analysis was performed on the NWR elicited by electrical stimulation on the sole of the foot. The analysis is based on decomposition of electromyographic (EMG) signals and is intended to describe the coordinated action between the muscles, describing their temporal activation profiles along with their relative weights (Ivanenko et al., 2016).

EXPERIMENTAL PROCEDURES

Sixteen healthy volunteers (nine males, range 20-35 years) participated in the study. The study protocol was approved by the Region Nordjylland (Denmark) ethical committee (case number VN 2015-0038). All subjects gave their written informed consent before participating in the study.

EMG recordings

Surface EMG signals were recorded from two distal muscles, tibialis anterior (TA) and soleus (SOL), and two proximal muscles, biceps femoris (BF) and rectus femoris (RF). The electrodes (type 720, Ambu A/S, Denmark) were placed 20 mm apart over the belly of each of the four muscles along the main direction of the muscle fibers. Electrodes were located following the recommendations of surface EMG for Non-Invasive Assessment of Muscles (SENIAM) (Hermens et al., 2000) in a single differential configuration. The skin was cleaned and lightly abraded before the placement of the electrodes in order to decrease electrode impedance. EMG signals were sampled at 2400 Hz, amplified (up to 20000 times), band-pass filtered (5-450 Hz), displayed and stored between 500 ms before stimulation and 2000 ms after stimulation.

Electrical Stimulation

Transcutaneous electrical stimulation was applied on the arch of the foot by a computer-controlled electrical stimulator (Noxitest IES 230, Aalborg University, Denmark) through a self-adhesive cathode (type 700, 20 x 15 mm, Ambu A/S, Denmark). A large anode electrode (50 x 90 mm, Pals, Axelgaard Ltd., Fallbrook, California, USA) was placed on the dorsum of the foot, to ensure that nociceptors were activated at the arch of the foot (Frahm et al., 2013). Each stimulus consisted of a constant-current burst of five individual 1-ms pulses delivered at 200 Hz, which the subjects perceived as a single stimulus located in the arch of the foot. Stimulation was delivered at random inter-train interval lengths ranging from 8 to 10 s. To ensure the presence of reflexes, the stimulation intensity was set to two times the reflex threshold (RTh) and assessed on the BF muscle (see below).

Experimental design

Initial setup

Subjects were placed in an articulated bed in a supine position, with their knees flexed approximately 30^{o} relative to the horizontal level and with back support in 120^{o}. To minimize

potential effects of arousal or anxiety on the NWR responses, subjects were thoroughly familiarized with electrical stimulation by applying multiple stimulations at different intensities before data were recorded.

Thresholds to electrical stimulation and NWR detection

The RTh to single stimulation was determined in the BF muscle using a standardized staircase procedure, with a detection / non-detection criterion (see below), and controlled by custom-made software. First, stimuli were administered with increasing intensity using steps of 2 mA until a NWR was detected. Second, the intensity was decreased in steps of 1 mA until the NWR was not detected. Four more staircase reversals were obtained with 1-mA steps, and the RTh was defined as the average intensity of the last three reversals (Arguissain et al., 2015).

The criterion to detect the presence of a NWR in the BF muscle was the interval peak z-score (Rhudy and France, 2007). The interval peak z-score was obtained from the rectified EMG and calculated as the difference between the peak amplitude in the reflex quantification interval of the BF muscle (60 - 180 ms post-stimulation) and the baseline amplitude mean (120 - 0 ms pre-stimulation), divided by the standard deviation of the baseline amplitude. A NWR was detected when the interval peak z-score was larger than 12 (Rhudy and France, 2007; Biurrun Manresa et al., 2011).

Experimental design

Figure 1 shows a schematic of the experiment design. The experiment consisted of a single session divided into 3 blocks: *Pre-CPM*, *During-CPM* and *Post-CPM*.

Pre-CPM and *Post-CPM*: subjects were asked to immerse their right hand, wide open up to the wrist, in a lukewarm bath (30.3 ± 0.7 °C), with a circulating water flow.

During-CPM: the cold pressor test (CPT) was used as the conditioning stimulus (CS), which was performed by immersing the subject's right hand, wide open up to the wrist, in a bucket with ice water (2.7 ± 0.5 °C), with a circulating water flow. The bucket had an inner and an outer compartment separated by a mesh screen to prevent direct contact between the ice and the hand. Subjects maintained the hand in the water bath for as long as they could tolerate it, or for a maximum period of 3 min.

In each block, ten electrical stimuli were delivered on the arch of the foot to elicit NWRs. Before and after the immersion of the hand in the water, skin temperature was monitored to ensure that the skin temperature before the Pre-CPM and Post-CPM blocks was similar. A resting period of 5 to 7 min was included between blocks.

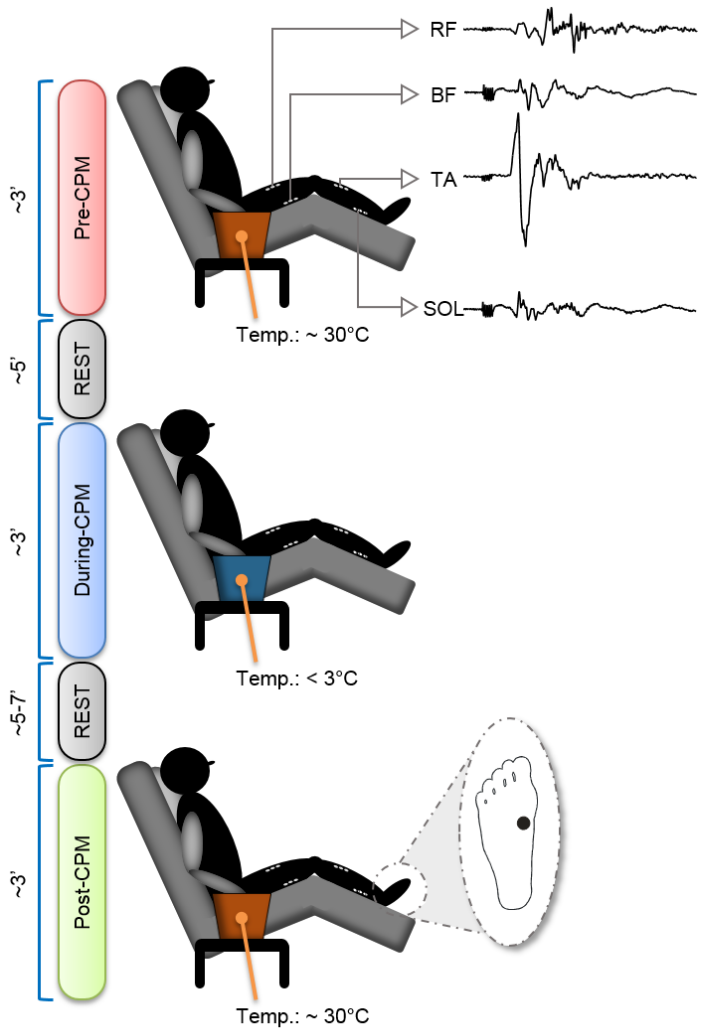

Fig. 1 Experimental design. Subjects were sitting on a comfortable adjustable bed with back and knee support. Electrical stimulation was delivered at the arch of the sole of the foot in order to elicit the NWR. The EMG of four muscles were recorded (RF, rectus femoris; BF, biceps femoris; TA, tibialis anterior; SOL, soleus). The experimental session was split in three blocks (Pre-CPM, During-CPM and Post-CPM) each one lasting approximately three minutes with a short rest between blocks. During blocks, subjects were asked to put their left hand into a water bath at different temperatures according to the block.

Data Analysis

CPM effect

Since the main objective was to observe the effects of CPM over the NWR pattern, only subjects who positively responded to the CPM effect (i.e. inhibition of the NWR) were further included in the EMG decomposition analysis. In order to quantify the CPM effect, the magnitude of the EMG activity of the BF muscle was calculated as the root-mean-square (RMS) in the reflex quantification interval. The across-trial average RMS of the BF muscle was obtained for each subject and each experimental block.

Muscle synergy analysis

EMG signals were high-pass filtered (digital zero-phase, fourth-order Butterworth filter, 50Hz cutoff) to clean it from motion artifacts (Cheung et al., 2009). Subsequently, the signals were rectified and low-pass filtered (digital zero-phase, fourth-order Butterworth filter, 20Hz cutoff) to obtain the EMG envelopes (d'Avella et al., 2006; Cheung et al., 2009).

For the EMG decomposition, a post-stimulus reflex window was chosen between 60 and 250ms to capture the concurrent activity of all recorded muscles. The median of the EMG envelopes was calculated per muscle, block and subject. After offset level subtraction, envelopes were normalized to the median of the maximum values across blocks.

Muscle synergies were further extracted, per subject and block, by decomposing the obtained EMG envelopes using a non-negative matrix factorization (NMF) algorithm (Lee and Seung, 1999, 2001; Tresch et al., 1999). Each muscle activation pattern can be reconstructed as a linear combination of spatial muscle synergies, known as *time-invariant synergies*. This reconstruction is defined as:

$$\boldsymbol{EMG} = \boldsymbol{WC} + \boldsymbol{e_m} \qquad \text{(Eq. 1)}$$

where $\boldsymbol{EMG}$ is a $m \times t$ matrix containing EMG measures (m number of muscles; t time points); $\boldsymbol{W}$ is a $m \times s$ muscle weights matrix, which represents the fixed (time-invariant) muscular contribution to each module (s number of synergistic modules); $\boldsymbol{C}$ is an $s \times t$ time-varying coefficient matrix, which represents the time activation of each module; and $\boldsymbol{e_m}$ is the residual

matrix. All elements are constrained to be non-negative, as muscle activation by definition is a positive variable. In principle, $\boldsymbol{W}$, $\boldsymbol{C}$ and *s* are unknown parameters.

To obtain $\boldsymbol{W}$ and $\boldsymbol{C}$, the algorithm randomly initialized all values, which converged to a local solution of the factorization in Eq. 1 (Lee and Seung, 2001). To avoid local minima, the algorithm was run 1000 times for each subject and block. The best reconstruction of the original EMG was kept based on the minimization of the mean squared error (MSE) between the reconstructed patterns and the original EMG signal (Frère and Hug, 2012).

This process was repeated between 1 and *m* times, and the first iteration that accounted for over 90 % of 'variance accounted for' (VAF) was the one that defined the minimum number of module synergies *s* that could explain the original EMG signals (Torres-Oviedo, 2006).

The "centered" VAF is defined as:

$$VAF = 1 - \frac{\|e_m\|_F^2}{\|EMG - \overline{EMG}\|_F^2} \quad \text{(Eq. 2)}$$

where $\|\cdot\|_F$ denotes the Frobenius norm of a matrix (Frère and Hug, 2012; Wojtara et al., 2014), and $\overline{EMG}$ represents the mean vector of each row in EMG (d'Avella et al., 2006). In order to define the number of synergies s with this ad-hoc criterion, it was considered that the total variability of all subjects per experimental block had to be above the 90% VAF threshold (Kristiansen et al., 2015).

Once *s*, $\boldsymbol{W}$ and $\boldsymbol{C}$ were defined, the obtained matrices were used to reconstruct the individual muscle pattern that took part in each synergistic module for each muscle. The muscle patterns were defined by the product of the muscle weights and the time activation of each synergistic module. The reconstructed EMG signals was then defined as the sum of the muscle patterns. The RMS of the individual muscle patterns and the reconstructed EMG signals was calculated on the aforementioned time window of interest (between 60 and 250 ms) for each subject and for each experimental block.

Statistics

CPM effect

To assess the CPM effect, non-parametric Friedman ANOVA was performed to compare the NWR sizes, with '*Condition*' as a factor (*Pre-CPM, During-CPM* and *Post-CPM*). Post hoc non-parametric Wilcoxon tests were used in case of significant effect. The comparisons considered were between the *Pre-CPM* and the *During-CPM* blocks, and between *Pre-CPM* and *Post-CPM* blocks.

Time-varying coefficients

For each synergistic module found, a point-by-point Wilcoxon rank-sum two-tailed test using a permutation strategy (1000 permutations) and a maximum cluster threshold of 97.5 was applied between *Pre-CPM* and *During-CPM* conditions and between *Pre-CPM* and *Post-CPM* conditions.

Muscle weights

Two-way repeated measure analysis of variance (RM ANOVA) was used for each synergistic module found, to test the effect of CPM on the muscle weights. The main factors were *Condition* (*Pre-CPM; During-CPM; Post-CPM*) and *Muscle* (*TA – SOL – BF – RF*). The Greenhouse-Geisser correction was applied to compensate for deviations in sphericity.

Muscle Patterns and Reconstructed EMG

For each synergistic module and for each reconstructed EMG, non-parametric Friedman ANOVA was performed to compare the RMS of the muscle patterns, with '*Condition*' as a main factor (*Pre-CPM, During-CPM* and *Post-CPM*). Post hoc non-parametric Wilcoxon tests were used in case of significant effects. The comparisons considered were between the *Pre-CPM* and the *During-CPM* blocks, and between *Pre-CPM* and *Post-CPM* blocks.

In all statistical tests, a *p*-value smaller than 0.05 was regarded as significant. Bonferroni correction was used to account for multiple comparisons.

RESULTS

The mean RTh intensity across all subjects measured in the BF muscle was 8.62 ± 4.51 mA (range 3 – 18 mA), so the mean stimulation intensity used was 17.23 ± 9.03mA (range 6 – 36 mA).

A primary screening of the dataset showed that 35 out of 1920 (1.82%) observations had to be eliminated due to voluntary contractions or technical problems.

CPM effect

The rectified EMG activity of the BF, averaged across subjects for the three different blocks, is shown in fig. 2 A (Pre-CPM, red; During-CPM, blue; Post-CPM, green). A pre-analysis of the dataset revealed that four out of sixteen subjects tested did not show NWR inhibition during the CS (Fig. 2, B). As the focus of this study was to describe the NWR pattern in terms of muscle synergies under CPM, these subjects were excluded from the analysis.

A significant main effect of *Condition* was found for the RMS of the BF muscle ($X^2 = 11.167$, $p = 0.004$). The post hoc analysis showed that the NWR measured in the BF were smaller when subjects had their hand in the ice-cold water bath (*During-CPM*) in comparison to when they had their hand in lukewarm water at the beginning of the experiment (*Pre-CPM*) ($Z = 3.059$; $p < 0.01$). No significant modulation was detected in the post-CS recording (Fig. 2, C).

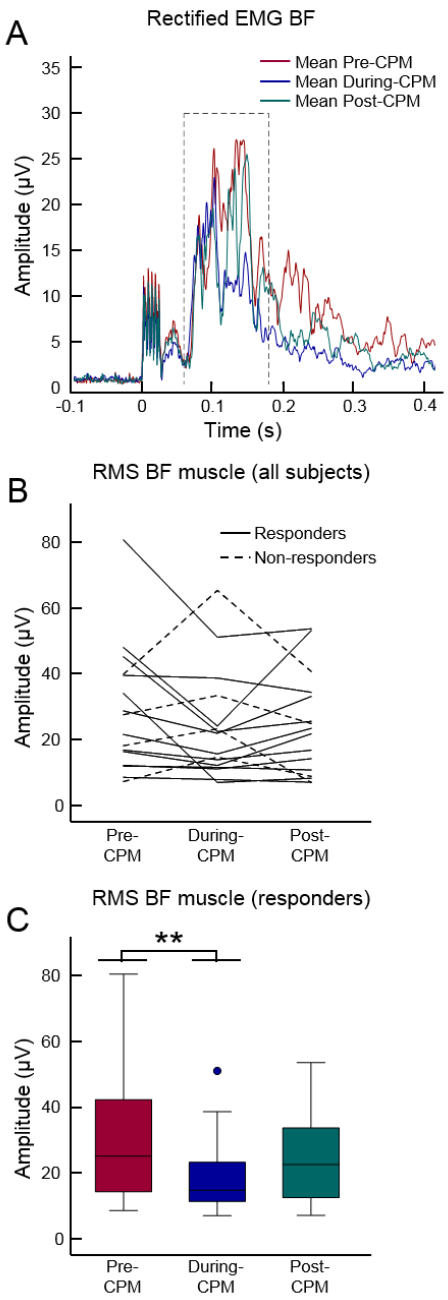

Fig. 2 CPM effect on BF muscle. (A) Figure shows the average across subjects rectified EMG of the BF for the three different blocks (Pre-CPM, red; During-CPM, blue; Post-CPM, green). The dotted square specifies the reflex quantification window of the BF muscle (60-180ms post stimulus). (B) Lines describe the mean RMS of the NWR measured in the BF muscle for each subject and block. The CPM non-responders (dotted line) were excluded from the muscle synergy analysis. (C) Boxplots describe the mean RMS of the NWR measured in the BF muscle in the quantification window considering only CPM responding subjects. A significant difference was found between Pre-CPM and During-CPM ($p < 0.01$).

Muscle Synergies

Number of extracted Module Synergies

Figure 3 displays the %VAF across subjects as a function of the number of synergy modules, for each experimental block. As it can be observed, two module synergies explain more than 90% of the VAF in the majority of the cases (i.e. experimental blocks per subjects). Although, there are few cases (8/36) where the 90% threshold was not reached. However, a third module synergy would explain less than 8% of the variance. In addition, the withdrawal reflex elicited from a resting position is expected to be a simple movement. Therefore, the muscle weights $\boldsymbol{W}$ and the time-varying coefficients $\boldsymbol{C}$ with two module synergies (s = 2) were further considered for the analysis. Consequently, Eq. 1 is expressed as follows:

$$\begin{bmatrix} EMG_{m_1 t_{60ms}} & \cdots & EMG_{m_1 t_{250ms}} \\ \vdots & \ddots & \vdots \\ EMG_{m_4 t_{60ms}} & \cdots & EMG_{m_4 t_{250ms}} \end{bmatrix} = \begin{bmatrix} w_{m_1 s_1} & w_{m_1 s_2} \\ \vdots & \vdots \\ w_{m_4 s_1} & w_{m_4 s_2} \end{bmatrix} \begin{bmatrix} c_{s_1 t_{60ms}} & \cdots & c_{s_1 t_{250ms}} \\ c_{s_2 t_{60ms}} & \cdots & c_{s_2 t_{250ms}} \end{bmatrix} + \boldsymbol{e_m} \quad \text{(Eq.3)}$$

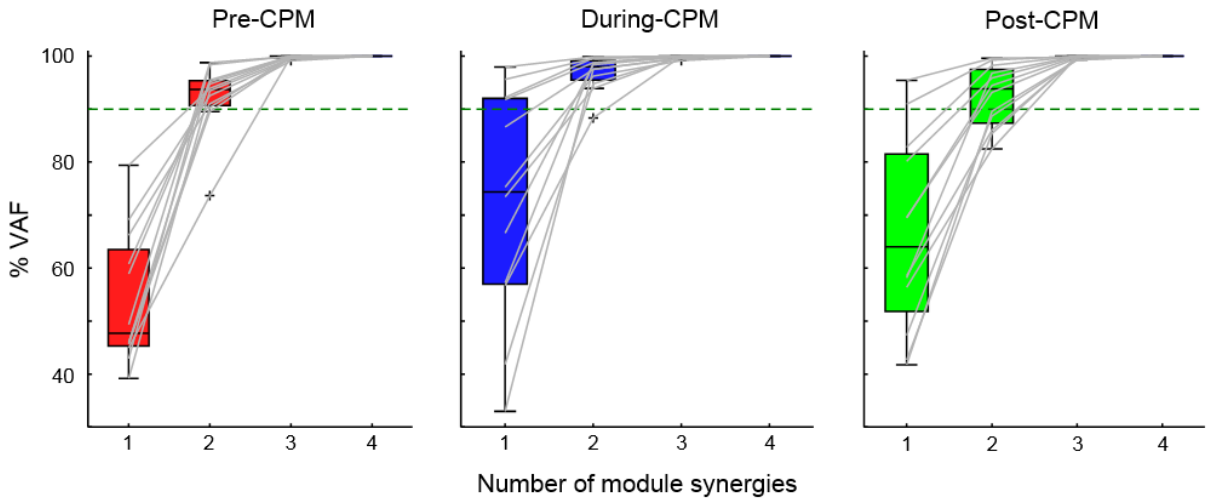

Fig. 3 Number of Module synergies. Boxplots describe the 'variance accounted for' (%VAF) across subjects for the three different blocks (Pre-CPM, red; During-CPM, blue; Post-CPM, green). Gray lines represent the individual responses. For the three different situations, the minimum number of module synergies that was considered for the population tested was two.

Time-varying coefficients

Figure 4 displays the two module synergies (Module I and II) for the three experimental blocks. Module I displayed an early component that presented a maximum amplitude around 90-110 ms. Module II displayed a late component with a latency onset around 120 ms and a maximum amplitude around 140-220 ms.

For Module I, a significant decrement of the time-varying coefficient was found in the time interval between 118-156 ms *During-CPM* in comparison with *Pre-CPM*. In other words, subjects had a smaller activation of Module I when they kept their hand in the ice-cold water bath in comparison with when they had their hand immersed in the lukewarm bath at the beginning of the experiment. Furthermore, a significant decrement of the time-varying coefficient was found in the time interval between 187-222 ms *Post-CPM* in comparison with *Pre-CPM*. Thus, subjects had a smaller activation of Module I when they had their hand immersed in the lukewarm bath, after the conditioning block, in comparison with the beginning of the experiment.

For Module II, a significant decrement on the time-varying coefficient was found in the time interval between 150-250 ms *During-CPM* in comparison with *Pre-CPM*. In other words, subjects had a smaller activation of Module II when they had their hand in ice-cold water bath in comparison with lukewarm water bath. No further significant effects were found.

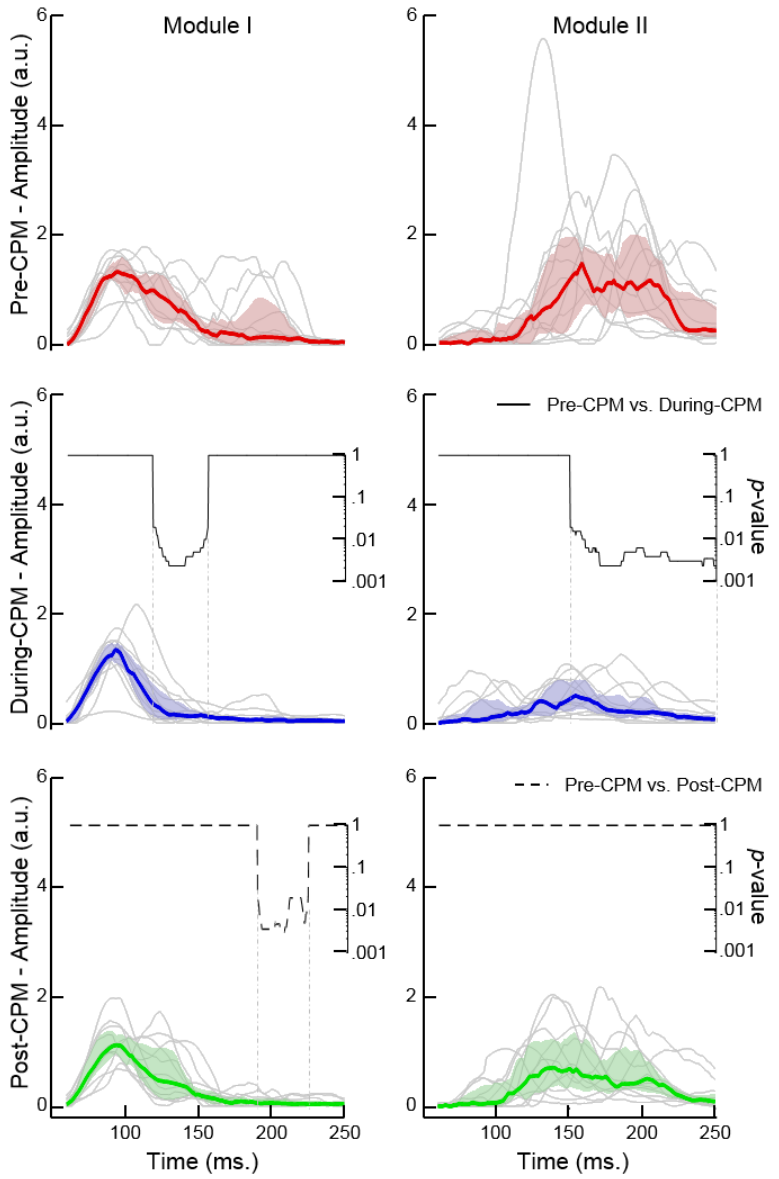

Fig. 4 Module Synergies - Time varying coefficients. Figure describes the two found module synergies decomposed in the time varying coefficients for the three different blocks (Pre-CPM, red; During-CPM, blue; Post-CPM, green). Gray lines represent the subject individual activations coefficients, full colored lines represent the median and the shades indicate the 25-75 percentile. *Module I*: A decrement in the time-varying coefficient was found between 118-156 ms post-stimulus interval (*p*-value is shown in black full line), when participants were subjected to the conditioning stimulus. In addition, an after-effect can be seen between 187-222 ms post-stimulus interval (*p*-value is shown in black slashed line). *Module II*: Due to the conditioning, a decrement in time-varying coefficient was found between 150-250 ms post-stimulus interval (*p*-value is shown in black full line), no further significant effects were found.

Muscle weights

For Module I, a significant main effect of *Muscle* was found ($F_{G\text{-}G}(3,33) = 21.531$, $p < 0.001$), whereas no further differences were found due to *Condition* or interactions. The post-hoc analysis showed a minor level of contribution of the RF muscle in comparison with the contributions of TA ($p < 0.001$), SOL ($p < 0.001$), and BF ($p < 0.001$) muscles (Fig. 5, A).

For Module II, a significant main effect of *Muscle* was found ($F_{G\text{-}G}(3,33) = 15.659$, $p < 0.001$). A post-hoc analysis indicated a predominant contribution of RF muscle in comparison with the contributions of TA ($p < 0.001$), SOL ($p < 0.001$), and BF ($p < 0.05$) muscles. In addition, the BF muscle presented a higher level of contribution compared to the TA muscle ($p < 0.01$). The analysis showed no further differences due to *Condition* or Interactions (Fig. 5, B).

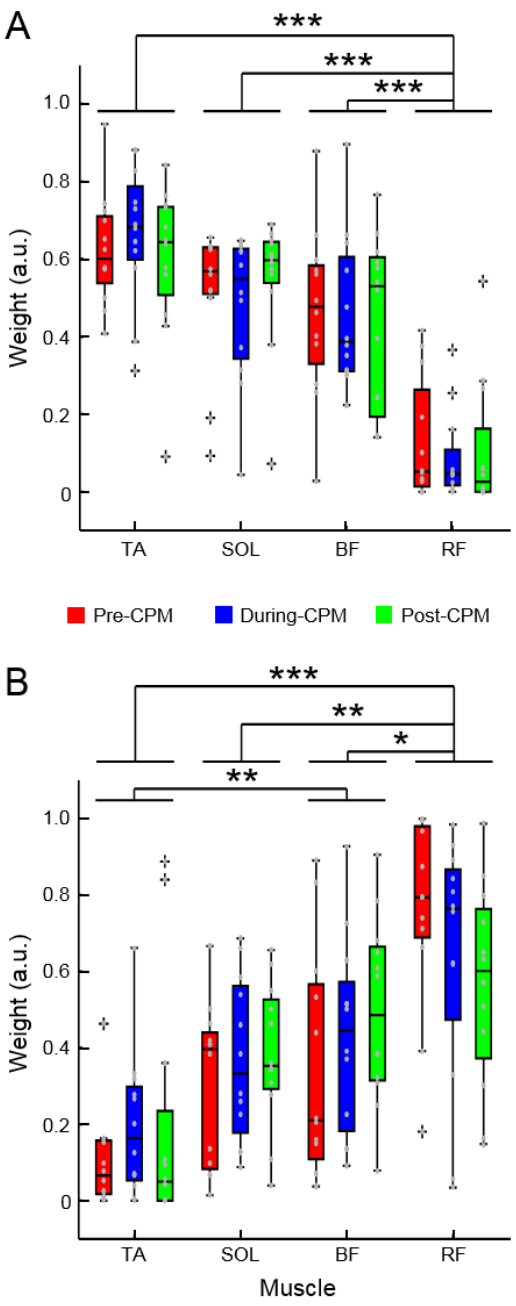

Fig. 5 Module Synergies – Muscle weights. Boxplots describes the two module synergies found (Module I and II) decomposed in the muscle weights for the three different blocks (Pre-CPM, red; During-CPM, blue; Post-CPM, green; gray dots indicate the subject individual weights), for the four muscles analyzed (TA, SOL, BF and RF). (A) The muscles weights analysis showed a minor contribution of RF muscle in comparison with the rest of the involved muscles ($p < 0.001$). (B) The muscles weights analysis showed a predominant contribution of RF muscle in comparison with TA ($p < 0.001$), SOL ($p < 0.01$) and BF ($p < 0.05$) muscles. In addition, a higher contribution of BF muscle was observed in comparison with TA ($p < 0.01$) muscle.

Muscle Patterns and Reconstructed EMG

The RMS of the individual muscle patterns for each module synergy are shown in Figure 6. The RMS analysis of the muscle patterns of Module II showed a significant main effect of *Condition* (X^2 = 9.50, $p_{Bonferroni\text{-}corrected}$ = 0.035) over the reconstructed pattern of the RF muscle. A post hoc analysis indicated that, in regards to the Module II, the RF muscle activation was smaller when subjects were under the conditioning stimulus (p < 0.01). No further differences were found.

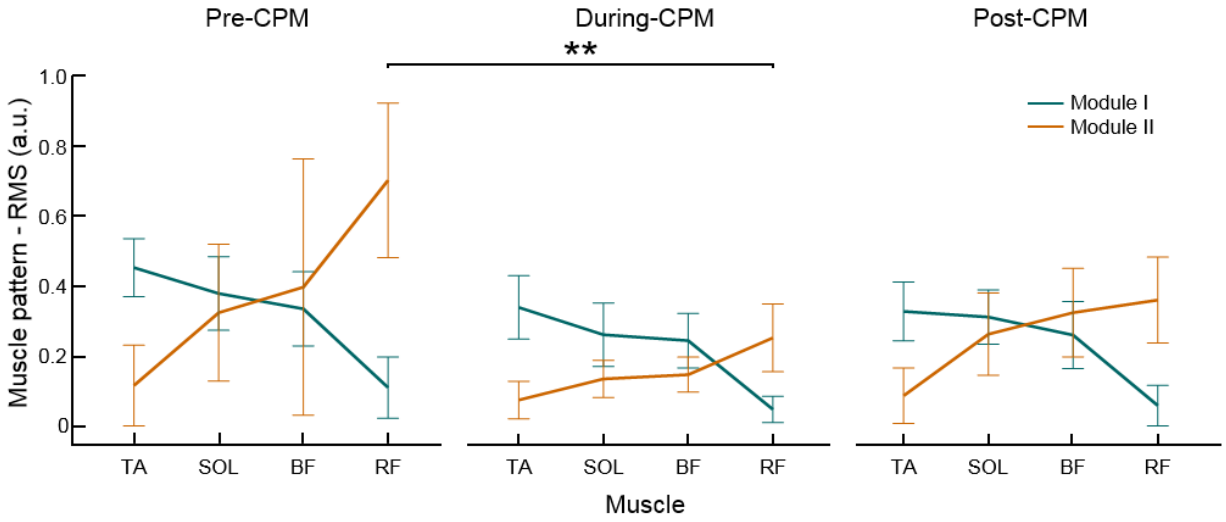

Fig. 6 RMS of the individual muscle patterns per module synergy. Lines describes the average and error bars represent the 95% CI of the RMS of the muscle patterns, per muscle (TA, SOL, BF and RF), for the two module synergies found (Module I, dark green; Module II, orange) and for each of the experimental blocks (Pre-CPM, During-CPM and Post-CPM). The RMS analysis indicated a significant decrement of the RMS size of the RF muscle pattern for Module II, when subjects were exposed to the conditioning stimulus (p < 0.01).

Figure 7 shows the individual muscle patterns (A) that were part of each synergistic module (Module I and II), together with the reconstructed EMG (B) for each muscle. A significant main effect of *Condition* was found for the BF (X^2 = 10.17, $p_{Bonferroni\text{-}corrected}$ = 0.025) and RF (X^2 = 14.00, $p_{Bonferroni\text{-}corrected}$ = 0.004) muscles in the RMS of the reconstructed EMG. A post hoc analysis showed that the NWR was smaller in the BF (p < 0.05) and the RF muscles (p < 0.01), when subjects kept their hand in the ice-cold water bath in comparison with when they had their hand immersed in the lukewarm bath at the beginning of the experiment. Furthermore, the NWR

of the RF muscle was also smaller ($p < 0.05$) when subjects had their hand immersed in the lukewarm bath, after the conditioning block, in comparison with the beginning of the experiment. The analysis showed no further differences.

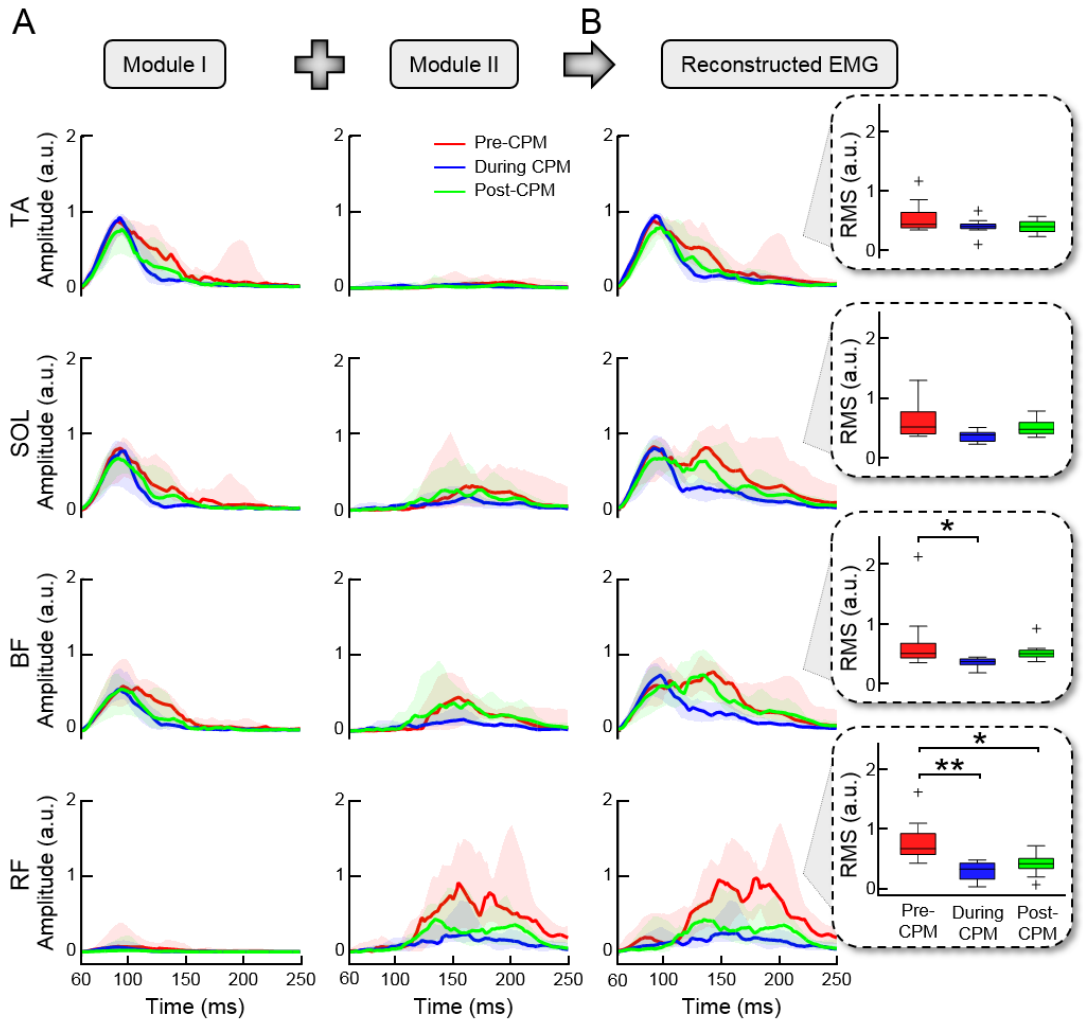

Fig. 7 Muscle patterns and reconstructed EMG. Figure describes the individual muscle activation patterns for two module synergies found (A) and the reconstructed EMG (B), for the three different blocks (Pre-CPM, red; During-CPM, blue; Post-CPM, green; full colored lines represent the median and the shades indicate the 25-75 percentile), for the four muscles analyzed (TA, SOL, BF and RF). The RMS analysis of the reconstructed EMG showed a significant decrement on BF ($p < 0.05$) and RF ($p < 0.01$) muscles when subjects kept their hand in cold water in comparison with the Pre-CPM block. Furthermore, a significant decrement of the RF activity ($p < 0.05$) was found when subjects kept their hand in lukewarm water in comparison with the Pre-CPM block. TA and SOL muscles did not show significant differences between blocks.

DISCUSSION

This study aimed to characterize the withdrawal pattern of lower limb during CPM. A muscle synergy analysis was performed based on the activation two distal (TA and SOL) and two proximal (RF and BF) muscles. Results indicate that the NWR response to electrical stimulation on the sole of the foot can be reconstructed by a linear combination of two muscle synergies (Module I and II). Module I presented an early activation profile with a maximum amplitude around 90-110ms, which included a minor contribution of RF muscle in comparison with the other muscles. On the contrary, Module II presented a late activation profile with a maximum amplitude around 140-220ms, which included a major contribution of RF muscle in comparison with the other muscles and a higher muscular contribution of BF muscle in comparison with TA muscle. Additionally, results suggest a differential modulatory effect on these synergies during CPM. Module I presented a significant reduced activation amplitude in a narrow time-window interval (118-156ms), whereas Module II presented a significant reduced activation amplitude in a wider time-window interval (150-250ms) under CPM. Furthermore, the analysis of the activation of the individual muscle patterns showed that the later activation of the RF was the most modulated reaction during CPM. Finally, the results suggest that the descending inhibitory drive affects mainly the muscles implicated in the knee and hip flexion.

Assessment of Conditioning Pain Modulation

Since Le Bars et al. in 1979 first described the ‘pain-inhibits-pain’ phenomenon in animals, named diffuse noxious inhibition control (DNIC), several experimental studies have investigated its behavioral correlate in humans, named CPM. These studies have consistently shown that a heterotopic noxious conditioning stimulus produces an inhibition of the spinal nociceptive reflexes (Willer et al., 1984, 1989; Le Bars et al., 1991; Terkelsen et al., 2001; Serrao et al., 2004; Biurrun Manresa et al., 2014). This modulation of the excitability of the nociceptive system at spinal level is believed to target mainly wide dynamic range (WDR) neurons in the dorsal horn (Schouenborg and Dickenson, 1985).

The role of neurotransmitters such as opioids and amines in spinal and supraspinal systems under CPM is still under debate. Literature showed mixed results about the role of the opioidergic system in CPM (Suzan et al., 2013). While some studies reported that administering an opioid antagonist (i.e. naloxone) can block the CPM effect (Willer et al., 1990; Sprenger et al., 2011), other studies did not find such effects (Peters et al., 1992; Edwards et al., 2004). A

possible explanation for the differences might be the type of CS paradigm employed to elicit CPM.

The assessment of the NWR size of the BF muscle indicated an inhibition during CPM. Thus, during the CS, a depression of the reflex size was observed, suggesting that the descending inhibitory mechanisms of CPM were triggered. Furthermore, the BF response measured 5-7 min after the CS was not significantly different from the response at beginning of the experiment, which indicates that the obtained effect was due to the conditioning rather than a general habituation of the NWR.

Noteworthy, four out of the sixteen tested subjects in the present study were considered CPM non-responders and therefore were excluded for the synergy analysis. Those subjects presented an enhancement of the NWR RMS under the CS, instead of a decrement or an absence of the response. Similar observations have been reported for the CPM paradigm in healthy subjects, where ~10% of CPM non-responders was found (Locke et al., 2014). A more recent report states that the number of non-responders using CPT as CS for CPM paradigm was between 11.5% and 46.2% of the tested subjects, across different test stimuli, and depending on the definition of CPM the quantity of non-responders could raise up to 75% (Vaegter et al., 2018). Still, it is likely that there is a continuous spectrum of the magnitude of the CPM effect, which is probably dependent on the individuals' variability and the CPM paradigm employed (Kennedy et al., 2016). Interestingly, it has been proposed that subjects displaying low-efficiency CPM could express a higher pain phenotype, which could lead to a higher risk of developing chronic pain (Yarnitsky et al., 2014). Studying CPM is relevant because CPM impairments have been speculated as mechanisms involved in the chronification of pain (Yarnitsky, 2010).

Interpretation of the NWR synergies

The present reflex observations suggest that at least two synergies are needed to describe the withdrawal pattern of the leg due to nociceptive stimulation on the arch of the foot, reconstructed from the activity of two distal (TA, SOL) and two proximal (BF, RF) muscles. These synergies were identified within the late - nociceptive - component interval of the reflex (RIII, 60-250 ms), and are differentiated by the time activation profiles but also the specific muscle contributions. Module I mainly presents an early component with a latency onset starting at 60 ms, and a maximum activation response within 90-110 ms after stimulation onset. This module had a major contribution of the TA, followed by the SOL and BF with negligible activity from the RF. On the

other hand, Module II presents a late component with a latency onset at 120 ms and a maximum activation response between 140-220 ms after stimulation. This module presents a major contribution of the RF and BF followed by activation of the SOL, with negligible activity from the TA.

The time activation of these two synergies well corresponds to the temporal profiles of EMG activity of muscles involved in the NWR that were reported in previous studies. In these studies, the NWR was generally dissociated into an early (50 to 120 ms) and a late (120 to 200 ms) reflex component (Grimby, 1963; Shahani and Young, 1971; Willer, 1977; Meinck et al., 1985; Roby-Brami and Bussel, 1987; Dowman, 1991). In addition, the contribution of each muscle (i.e. weights) to the two synergies seems to be in agreement with the activation pattern the different muscles have in the two reflex components reported in the literature (Sonnenborg et al., 2001). Specifically, the TA muscle (a distal dorsal flexor) generally presents a single burst of activity with an onset latency that corresponds to the early component of the NWR (Arguissain et al., 2015), whereas the SOL muscle (a distal ankle extensor) presents a clear double burst with onset latencies that correspond to the early and late components, respectively (Andersen et al., 1999). Furthermore, the BF usually presents a single burst that extends across the time window of the two reflex components (Willer et al., 1989), whereas the RF muscle (a proximal hip flexor) has a single burst that is present in the late stage of the reflex (Roby-Brami and Bussel, 1987; Decchi et al., 1997). Altogether, the two synergistic modules could be interpreted as the muscle group actions that are involved in the biomechanical reaction to a noxious stimulus on the medial part of the plantar side of the foot (Andersen et al., 1999). Particularly, Module I may characterize the immediate protective reaction to the noxious stimulus, preferentially involving distal joints (i.e. a recruitment of the TA muscle for the dorsiflexion of the foot and a recruitment of the SOL muscle for the stabilization of the ankle joint). In addition, the substantial activation of the BF muscle seen for Module I might indicate an early knee-flexion, as a limb preparation. Alternatively, Module II may characterize the withdrawal reinforcement, preferentially involving proximal joints (i.e. a recruitment of BF muscle for a stabilization of the knee joint and a recruitment of the RF muscle for a hip-flexion). Moreover, the high activation of the SOL muscle seen for Module II might suggest the unloading of the ankle joint.

CPM effect on NWR synergies

A substantial depression of the time activation of Module II was observed under CS. This modulation was detected between 150-250 ms, comprising the area of maximum activation

response for this synergy module component. The effect observed in Module II, which preferentially comprises the activation of proximal muscles, is in line with previous studies that investigated descending modulation of spinal excitability with the BF activity as main outcome measurement (Willer et al., 1984, 1989; Le Bars et al., 1991; Terkelsen et al., 2001; Serrao et al., 2004; Biurrun Manresa et al., 2014). Additionally, the time activation of Module I, which preferentially comprises the activation of distal muscles, was partially affected during CS. Noteworthy, the latter modulation was observed in the transition interval between the maximum amplitude of the two synergistic modules (118-156 ms), whereas the maximum activation response interval (90-110 ms) for this module remained unaffected. To the authors' knowledge, there are no previous studies that investigated the CPM effect in distal muscles in humans. Nevertheless, studies in animals have reported that NWR of different hindlimb muscles could be differentially modulated by descending pathways activated by a distant noxious stimulus (Kalliomäki et al., 1992; Morgan, 1999). Particularly, while the CS inhibited the NWR in the majority of hindlimb muscles, reflexes in e.g. the plantar flexors of the digits were facilitated (Kalliomäki et al., 1992). This mechanism presumably reduces the chance of tissue damage by keeping the withdrawal capacity and escape reactions (Morgan, 1999).

A second possible explanation for the differential modulation of the modules time activation relates to the different types of afferents that mediate the NWR. In the literature, the nature of the different components of the NWR has been extensively discussed (see Sandrini et al. 2005 and Andersen 2007 for a review). Previous studies have described an early, inconstantly present component (RII, 40 – 60 ms) which is mediated by low-threshold, non-nociceptive Aβ-fibers. The late, always present components are mediated by nociceptive Aδ-fibers (RIII, 60-250 ms). Nevertheless, it is possible that both Aδ and Aβ afferent activity contribute to a different degree to the elicitation of these responses (Arcourt et al., 2017). In this study, the RII response was not included in the analysis due to its reported inconsistency (Hugon, 1973; Willer, 1977; Sandrini et al., 2005). Still, the NWR pattern presented an activity burst in the 60-250 ms time window, which was decomposed into two components by means of the synergy analysis. Therefore, the observed modulation of the Module II due to CS suggests that the late component of the NWR has a larger contribution of Aδ-fibers that are subjected to endogenous inhibitory modulation. Yet, further studies are still needed to clarify and identify the co-activation of these fibers.

Furthermore, the muscle weights showed no significant changes for either module due to CS. The fact that the muscle contributions were not modulated by CPM corroborates the modular organization nature of the withdrawal reflex suggested by Schouenborg and colleagues (Schouenborg and Kalliomäki 1990). The modular organization of the NWR, defined in terms of muscle synergies, has been previously described in animals (Tresch et al., 1999).

Notably, despite of the RMS analysis of the individual muscle patterns that showed only a significant difference for RF muscle for the Module II (Fig. 6), the analysis of the reconstructed EMG showed a significant decrement of the BF and RF muscles activity during the conditioning stimulus (Fig. 7). Noteworthy, the reconstructed EMG considers the combination of the muscle patterns from *Module I* and *Module II*. These observations suggest a complex interaction between the neural drive exerted into the spinal cord and the encoded muscle weights, where minor variations in the individual muscle patterns could result in a large effect of the complete muscle activity, ending in different degrees of withdrawal. It is the first time that the NWR is studied by means of synergistic analysis in humans. This analysis provided an integrative overview of the individual muscles acting together to achieve a common goal, and how the interaction of the activation time and the muscle contribution could involve a differential modulation of the net withdrawal.

Altogether, the synergy analysis reveals that the supraspinal inhibition exerted onto the spinal cord may differentially affect the muscles involved in the withdrawal pattern. The present results indicate that the proximal muscles might be more susceptible to supraspinal modulation (Fig. 7). Therefore, in potentially dangerous situations where pain could compromise escape, the nervous system may activate and balance the most efficient withdrawal pattern by differentially modulating the muscles to protect the tissue but still allowing escape reactions. The net reflex result reflects a hierarchical system in which the withdrawal pattern is established based on the available muscle synergies that generate a specific reaction (Bizzi et al., 2008); this system is under a complex differential descending control that reduces the chances of tissue injury in situations of multiple noxious inputs (Morgan, 1999).

Prospective neural mechanisms

Results in this study suggest that the withdrawal reaction was adjusted by descending inhibitory drives exerted onto the spinal cord during CPM. Studies in animals suggest that the modulation of the excitability of the nociceptive system at spinal level targets mainly wide dynamic range

(WDR) neurons in the dorsal horn (Schouenborg and Dickenson, 1985; Kalliomäki et al., 1992). Since monosynaptic *Ia* reflexes are not altered by a conditioning stimulus, these inhibitory effects are presumably exerted on some (not all) WDR neurons that are intercalated in the withdrawal reflex pathways (Kalliomäki et al., 1992). Interestingly, spinal interneurons also play a significant role in the activation of synergistic motor modules. By means of multi-electrode recordings in the spinal cord of spinalized frogs, Hart and Giszter (2010) showed that certain sets of interneurons are likely responsible of organizing individual spinal motor primitives. Taken together, it is possible that the differentiation between the recruitment of muscles (or group of muscles) during the elicitation of the NWR might happen at the WDR neurons, where the different synergistic modules are weighted according to several factors (i.e. supraspinal excitability, posture, etc.). Still, the specific spinal reflex pathways where the synergistic modules are imprinted for individual muscles in humans remain unknown.

Methodological considerations

In the present study, only four muscles were selected to perform the synergistic analysis of the reflexes elicited by electrical stimulation on the arch of the foot. This might be a low number of muscles to perform a synergy analysis. Steele and co-workers (2013) have indicated that the number of muscles under analysis entails an important factor in the identification of the number of module synergies involved, where the analysis of a subset of few muscles could lead to an over-estimation of the variance accounted for, resulting in a fewer module synergies selected. However, the authors suggest a few methodological strategies to account for a small number of muscles. For instance, selecting a subset of muscles where the large and dominant muscles are included could help to decrease the sensitivity of synergies to experimental constraints such as a few number of muscles being measured (Steele et al., 2013). In this study, the four muscles were selected based on the biomechanical functions of those muscles acting across the three principal joints in the lower limb. In a seated position (Fig. 1), a noxious stimulus coming from the arch of the foot generally produces a withdrawal of the limb towards the core of the body. This withdrawal assumes a dorsiflexion of the ankle joint along with a possible flexion of the knee and a further flexion of the hip (i.e. a dorsi-flexor (TA) and a plantar-flexor (SOL); a knee-flexor (BF) and knee-extensor (RF); and hip-flexor (RF) and a hip-extensor (BF)) (Andersen et al., 2001). Still, the effect of the conditioning stimulus (i.e. CPT) was evaluated on the same subset of muscles, providing new insights into how supraspinal modulation affects the motor programs encoded in the spinal cord.

ACKNOWLEDGMENTS

Author Contributions

F.A.J., J.A.B.M., O.K.A. conceptualized and designed the study; F.A.J. carried out the experiments and analyzed the data; F.A.J., F.G.A., J.A.B.M. and O.K.A. drafted the manuscript and critically reviewed it.

Funding

The study was supported by the Danish National Research Foundation [DNRF121].

Declarations of Interest

None.

REFERENCES

Andersen OK (2007) Studies of the organization of the human nociceptive withdrawal reflex: Focus on sensory convergence and stimulation site dependency. Acta Physiol 189:1–35.

Andersen OK, Sonnenborg F, Arendt-Nielsen L (1999) Modular organization of human leg withdrawal reflexes elicited by electrical stimulation of the foot sole. Muscle Nerve 22:1520–1530 Available at: http://doi.wiley.com/10.1002/%28SICI%291097-4598%28199911%2922%3A11%3C1520%3A%3AAID-MUS6%3E3.0.CO%3B2-V.

Andersen OK, Sonnenborg F, Arendt-Nielsen L (2001) Reflex receptive fields for human withdrawal reflexes elicited by non-painful and painful electrical stimulation of the foot sole. Clin Neurophysiol 112:641–649.

Anon (n.d.) The effect of distraction strategies on pain perception and the nociceptive flexor reflex (RIII reflex).

Arcourt A, Gorham L, Dhandapani R, Prato V, Taberner FJ, Wende H, Gangadharan V, Birchmeier C, Heppenstall PA, Lechner SG (2017) Touch Receptor-Derived Sensory Information Alleviates Acute Pain Signaling and Fine-Tunes Nociceptive Reflex Coordination. Neuron 93:179–193.

Arguissain FG, Biurrun Manresa JA, Mørch CD, Andersen OK (2015) On the use of information theory for the analysis of synchronous nociceptive withdrawal reflexes and somatosensory evoked potentials elicited by graded electrical stimulation. J Neurosci Methods 240:1–12 Available at: http://dx.doi.org/10.1016/j.jneumeth.2014.10.011.

Bartolo M, Serrao M, Gamgebeli Z, Amtmann D, Perrotta A, Padua L, Pierelli F, Nappi G, Sandrini G (2013) Modulation of the human nociceptive flexion reflex by pleasant and unpleasant odors. Pain 154:2054–2059.

Biurrun Manresa JA, Fritsche R, Vuilleumier PH, Oehler C, Mørch CD, Arendt-Nielsen L, Andersen OK, Curatolo M (2014) Is the conditioned pain modulation paradigm reliable? A test-retest assessment using the nociceptive withdrawal reflex. PLoS One 9:1–9.

Biurrun Manresa JA, Jensen MB, Andersen OK (2011) Introducing the reflex probability maps in the quantification of nociceptive withdrawal reflex receptive fields in humans. J Electromyogr Kinesiol 21:67–76.

Bizzi E, Cheung VCK, d'Avella A, Saltiel P, Tresch M (2008) Combining modules for movement. Brain Res Rev 57:125–133 Available at: http://linkinghub.elsevier.com/retrieve/pii/S0165017307001774.

Bizzi E, d'Avella A, Saltiel P, Tresch M (2002) Modular Organization of Spinal Motor Systems. 8:437–442.

Bjerre L, Andersen AT, Hagelskjaer MT, Ge N, Mørch CD, Andersen OK (2011) Dynamic tuning of human withdrawal reflex receptive fields during cognitive attention and distraction tasks. Eur J Pain 15:816–821.

Cheung VCK, Piron L, Agostini M, Silvoni S, Turolla A, Bizzi E (2009) Stability of muscle synergies for voluntary actions after cortical stroke in humans. Proc Natl Acad Sci 106:19563–19568 Available at: http://www.pnas.org/cgi/doi/10.1073/pnas.0910114106.

d'Avella A, Portone A, Fernandez L, Lacquaniti F (2006) Control of Fast-Reaching Movements by Muscle Synergy Combinations. J Neurosci 26:7791–7810 Available at: http://www.jneurosci.org/cgi/doi/10.1523/JNEUROSCI.0830-06.2006.

Decchi B, Zalaffi A, Spidalieri R, Arrigucci U, Troia AM Di, Rossi A (1997) Spinal reflex pattern to foot nociceptive stimulation in standing humans. 105:484–489.

Dowman R (1991) Spinal and supraspinal correlates of nociception in man. Pain 45:269–281 Available at: http://www.sciencedirect.com/science/article/B6T0K-486S868-FK/2/1719a37544e54941a95ba85577250c24%5Cnfile:///Z:/private/PhD/References/NWR/dowman1991.pdf.

Edwards RR, Ness TJ, Fillingim RB (2004) Endogenous Opioids, Blood Pressure, and Diffuse Noxious Inhibitory Controls: A Preliminary Study. Percept Mot Skills 99:679–687 Available at: http://journals.sagepub.com/doi/10.2466/pms.99.2.679-687.

Eklund K, Grimby L, Kugelberg E (1959) Nociceptive reflexes of the human foot. The plantar responses. Acta Physiol Scand 47:297–298.

Frahm KS, Morch CD, Grill WM, Lubock NB, Hennings K, Andersen OK (2013) Activation of peripheral nerve fibers by electrical stimulation in the sole of the foot. BMCNeurosci 14:116. do:114–116.

Frère J, Hug F (2012) Between-subject variability of muscle synergies during a complex motor skill. Front Comput Neurosci 6:1–13 Available at: http://journal.frontiersin.org/article/10.3389/fncom.2012.00099/abstract.

Grimby L (1963) Normal plantar response: integration of flexor and extensor reflex components. J Neurol Neurosurg Psychiatry 26:39–50 Available at: http://jnnp.bmj.com/cgi/doi/10.1136/jnnp.26.4.314.

Hagbarth KE (1960) Spinal withdrawal reflexes in human lower limbs. J Neurol Neurosurg Psychiatry 23:222–227.

Hagbarth KE, Finer BL (1963) The Plasticity of Human Withdrawal Reflexes to Noxious Skin Stimuli in Lower Limbs. Prog Brain Res 1:65–81.

Hart CB, Giszter SF (2010) A Neural Basis for Motor Primitives in the Spinal Cord. J Neurosci 30:1322–1336 Available at: http://www.jneurosci.org/cgi/doi/10.1523/JNEUROSCI.5894-08.2010.

Heinricher MM, Tavares I, Leith JL, Lumb BM (2009) Descending control of nociception: Specificity, recruitment and plasticity. Brain Res Rev 60:214–225 Available at: http://dx.doi.org/10.1016/j.brainresrev.2008.12.009.

Hermens HJ, Freriks B, Disselhorst-Klug C, Rau G (2000) Development of recommendations for SEMG sensors and sensor placement procedures. J Electromyogr Kinesiol 10:361–374.

Hugon M (1973) Exteroceptive Reflexes to Stimulation of the Sural Nerve in Normal Man. In: Human Reflexes, Pathophysiology of Motor Systems, Methodology of Human Reflexes, pp 713–729. S. Karger AG. Available at: https://www.karger.com/Article/FullText/394186 [Accessed June 28, 2018].

Ivanenko YP, d'Avella A, Lacquaniti F (2016) Muscle coordination, motor synergies, and primitives from surface EMG. Surf Electromyogr Physiol Eng Appl:158–179.

Kalliomäki J, Schouenborg J, Dickenson AH (1992) Differential Effects of a Distant Noxious Stimulus on Hindlimb Nociceptive Withdrawal Reflexes in the Rat. Eur J Neurosci 4:648–652.

Kennedy DL, Kemp HI, Ridout D, Yarnitsky D, Rice ASC (2016) Reliability of conditioned pain modulation: A systematic review. Pain 157:2410–2419.

Kristiansen M, Madeleine P, Hansen EA, Samani A (2015) Inter-subject variability of muscle synergies during bench press in power lifters and untrained individuals. Scand J Med Sci Sport 25:89–97.

Kugelberg E, Eklund K, Grimby L (1960) An electromyographic study of the nociceptive reflexes of the lower limb. Mechanism of the plantar responses. Brain 83:394–410.

Le Bars D, Dickenson AH, Besson J-M (1979) Diffuse noxious inhibitory controls (DNIC). I. Effects on dorsal horn convergent neurones in the rat. Pain 6:283–304 Available at: https://doi.org/10.1016/0304-3959(79)90049-6.

Le Bars D, Villanueva L, Willer JC, Bouhassira D (1991) Diffuse Noxious Inhibitory Controls (DNIC) in animals and in man. Acupunct Med 9:47–56 Available at: http://www.ncbi.nlm.nih.gov/pubmed/1303506.

Lee DD, Seung HS (1999) Learning the parts of objects by non-negative matrix factorization. Nature 401:788–791 Available at: http://www.ncbi.nlm.nih.gov/pubmed/10548103.

Lee DD, Seung HS (2001) Algorithms for non-negative matrix factorization. Adv Neural Inf Process Syst:556–562 Available at: http://papers.nips.cc/paper/1861-algorithms-for-non-negative-matrix-factorization.

Lewis GN, Rice DA, McNair PJ (2012) Conditioned pain modulation in populations with chronic pain: A systematic review and meta-analysis. J Pain 13:936–944.

Locke D, Gibson W, Moss P, Munyard K, Mamotte C, Wright A (2014) Analysis of Meaningful Conditioned Pain Modulation Effect in a Pain-Free Adult Population. J Pain 15:1190–1198 Available at: https://www.sciencedirect.com/science/article/pii/S1526590014009080 [Accessed January 7, 2018].

Meinck HM, Küster S, Benecke R, Conrad B, K??ster S, Benecke R, Conrad B (1985) The flexor reflex—influence of stimulus parameters on the reflex response. Electroencephalogr Clin Neurophysiol 61:287–298.

Millan MJ (2002) Descending control of pain. Prog Neurobiol 66:355–474.

Morgan MM (1999) Paradoxical inhibition of nociceptive neurons in the dorsal horn of the rat spinal cord during a nociceptive hindlimb reflex. Neuroscience 88:489–498.

Peters ML, Schmidt AJM, Van den Hout MA, Koopmans R, Sluijter ME (1992) Chronic back pain, acute postoperative pain and the activation of diffuse noxious inhibitory controls (DNIC). Pain 50:177–187.

Rhudy JL, France CR (2007) Defining the nociceptive flexion reflex (NFR) threshold in human participants: A comparison of different scoring criteria. Pain 128:244–253.

Richard MA, Spaich EG, Serrao M, Andersen OK (2015) Stimulation site and phase modulation of the withdrawal reflex during gait initiation. Clin Neurophysiol 126:2282–2289 Available at: http://dx.doi.org/10.1016/j.clinph.2015.01.019.

Roby-Brami A, Bussel B (1987) Long-latency spinal reflex in man after flexor reflex afferent stimulation. Brain 110 (Pt 3:707–725 Available at: http://www.ncbi.nlm.nih.gov/pubmed/3107749.

Sandrini G, Serrao M, Rossi P, Romaniello A, Cruccu G, Willer JC (2005) The lower limb flexion reflex in humans. Prog Neurobiol 77:353–395.

Schouenborg J (2002) Modular organisation and spinal somatosensory imprinting. Brain Res Rev 40:80–91.

Schouenborg J, Dickenson A (1985) The effects of a distant noxious stimulation on A and C fibre-evoked flexion reflexes and neuronal activity in the dorsal horn of the rat. Brain Res 328:23–32 Available at: http://linkinghub.elsevier.com/retrieve/pii/0006899385913186 [Accessed January 7, 2018].

Schouenborg J, Kalliomäki J (1990) Functional organization of the nociceptive withdrawal reflexes. I. Activation of hindlimb muscles in the rat. Exp Brain Res 83:67–78.

Schouenborg J, Weng H, Holmberg H (1994) Modular Organization of Spinal Nociceptive Reflexes: A New Hypothesis. Physiology 9:261–265.

Schouenborg J, Weng HR (1994) Sensorimotor transformation in a spinal motor system. Exp brain Res 100:170–174 Available at: http://link.springer.com/10.1007/BF00227291.

Serrao M, Rossi P, Sandrini G, Parisi L, Amabile GA, Nappi G, Pierelli F (2004) Effects of diffuse noxious inhibitory controls on temporal summation of the RIII reflex in humans. Pain 112:353–360.

Shahani BT, Young RR (1971) Human flexor reflexes. J Neurol Neurosurg Psychiatry 34:616–627 Available at: http://www.ncbi.nlm.nih.gov/entrez/query.fcgi?cmd=Retrieve&db=PubMed&dopt=Citation&list_uids=5122389.

Sherrington CS (1910) Flexion-reflex of the limb, crossed extension-reflex, and reflex stepping and standing. J Physiol 40:28–121.

Sonnenborg F, Andersen OK, Arendt-Nielsen L, Treede RD (2001) Withdrawal reflex organisation to electrical stimulation of the dorsal foot in humans. Exp brain Res 136:303–312 Available at: http://link.springer.com/10.1007/s002210000587.

Spaich EG, Hinge HH, Arendt-Nielsen L, Andersen OK (2006) Modulation of the withdrawal reflex during hemiplegic gait: Effect of stimulation site and gait phase. Clin Neurophysiol 117:2482–2495.

Sprenger C, Bingel U, Büchel C (2011) Treating pain with pain: Supraspinal mechanisms of endogenous analgesia elicited by heterotopic noxious conditioning stimulation. Pain 152:428–439 Available at: http://dx.doi.org/10.1016/j.pain.2010.11.018.

Steele KM, Tresch M, Perreault EJ (2013) The number and choice of muscles impact the results of muscle synergy analyses. Front Comput Neurosci 7:105 Available at: http://www.ncbi.nlm.nih.gov/pubmed/23964232 [Accessed April 11, 2018].

Suzan E, Midbari A, Treister R, Haddad M, Pud D, Eisenberg E (2013) Oxycodone alters temporal summation but not conditioned pain modulation: Preclinical findings and possible relations to mechanisms of opioid analgesia. Pain 154:1413–1418 Available at: http://dx.doi.org/10.1016/j.pain.2013.04.036.

Terkelsen AJ, Andersen OK, Hansen PO, Jensen TS (2001) Effects of heterotopic- and segmental counter-stimulation on the nociceptive withdrawal reflex in humans. Acta Physiol Scand 172:211–217 Available at: http://eutils.ncbi.nlm.nih.gov/entrez/eutils/elink.fcgi?dbfrom=pubmed&id=11472308&retmode=ref&cmd=prlinks%5Cnpapers3://publication/uuid/18F16051-B40C-41CF-8C41-E9B39EDACC84%5Cnhttp://www.ncbi.nlm.nih.gov/pubmed/11472308.

Torres-Oviedo G (2006) Muscle Synergy Organization Is Robust Across a Variety of Postural Perturbations. J Neurophysiol 96:1530–1546 Available at: http://jn.physiology.org/cgi/doi/10.1152/jn.00810.2005.

Tresch M, Saltiel P, Bizzi E (1999) The construction of movement by the spinal cord. Nat Neurosci 2:162–167.

Vaegter HB, Petersen KK, Mørch CD, Imai Y, Arendt-Nielsen L (2018) Assessment of CPM reliability: quantification of the within-subject reliability of 10 different protocols. Scand J Pain:1–9 Available at: http://www.degruyter.com/view/j/sjpain.ahead-of-print/sjpain-2018-0087/sjpain-2018-0087.xml.

Willer JC (1977) Comparative study of perceived pain and nociceptive flexion reflex in man. Pain 3:69–80.

Willer JC, De Broucker T, Le Bars D (1989) Encoding of nociceptive thermal stimuli by diffuse noxious inhibitory controls in humans. J Neurophysiol 62:1028–1038.

Willer JC, Le Bars D, De Broucker T (1990) Diffuse noxious inhibitory controls in man: Involvement of an opioidergic link. Eur J Pharmacol 182:347–355.

Willer JC, Roby A, Bars D Le (1984) Psychophysical and electrophysiological approaches to the pain-relieving effects of heterotopic nociceptive stimuli. Brain 107:1095–1112.

Wojtara T, Alnajjar F, Shimoda S, Kimura H (2014) Muscle synergy stability and human balance maintenance. J Neuroeng Rehabil 11:1–9.

Yarnitsky D (2010) Conditioned pain modulation (the diffuse noxious inhibitory control-like effect): its relevance for acute and chronic pain states. CurrOpinAnaesthesiol 23:611–615.

Yarnitsky D, Granot M, Granovsky Y (2014) Pain modulation profile and pain therapy: Between pro- and antinociception. Pain 155:663–665 Available at: http://dx.doi.org/10.1016/j.pain.2013.11.005.